

Suomi-National Polar Orbiting Partnership (NPP) Calibration and Validation

The Suomi NPP (SNPP) satellite was launched successfully on October 28, 2011 and is a pathfinder for the future US Joint Polar Satellite System (JPSS) operational satellite series. The primary objectives of the SNPP mission are to continue the Earth system observations initiated by the Earth Observing System Terra, Aqua, and Aura missions and to prepare the operational forecasting community with pre-operational risk reduction, demonstration, and validation for selected JPSS instruments and ground processing data systems. The SNPP satellite is now flying with the following five instruments: (1) Visible/Infrared Imager/Radiometer Suite (VIIRS) has multi-band imaging capabilities to support the acquisition of high-resolution atmospheric imagery and generation of a variety of applied products including visible and infrared imaging of hurricanes and detection of fires, smoke, and atmospheric aerosols. (2) Cross-track Infrared Sounder (CrIS) is the first in a series of advanced operational sounders that provide more accurate, detailed atmospheric temperature and moisture observations for weather and climate applications. (3) Advanced Technology Microwave Sounder (ATMS) operates in conjunction with the CrIS to profile atmospheric temperature and moisture. The higher (spatial, temporal and spectral) resolution and more accurate sounding data of CrIS and ATMS support continuing advances in data assimilation systems and NWP models to improve short- to medium-range weather prediction. (4) Ozone Mapping and Profiler Suite (OMPS) measures the concentration of ozone in the atmosphere, providing information on how ozone concentration varies with altitude. Data from OMPS continue three decades of measurements of this important climate variable. The OMPS measurements also fulfill the U.S. treaty obligation to monitor global ozone concentrations with no gaps in coverage. (5) Cloud and Earth Radiant Energy System (CERES) seeks to develop and improve weather and models prediction, and to provide measurements of the space and time distribution of the Earth's Radiation Budget components. The observations from CERES are essential to understanding the effect of clouds on the earth's energy balance (energy coming in from the sun and radiating out from the earth), which is one of the largest sources of uncertainty in our modeling of the climate.

The SNPP instruments are now undergoing a period of intensive calval and the instrument on-orbit performances are stable and the post-launch results all meet or exceed the specifications (Figure 1 and Table 1). NOAA is in charge of calibration of four instruments: ATMS, CrIS, VIIRS and OMPS. The CrIS, ATMS and VIIRS Sensor Data Record (SDR) products have reached the provisional level at which users can order the data from NOAA (<http://www.class.ngdc.noaa.gov/saa/products/welcome;jsessi onid=CAA653564B301391746505E0E3E6EBB0>) and perform in-depth scientific research. Also, ATMS data have been operationally assimilated into global and regional forecast models, and a suite of Environmental Data Record (EDR) products is generated by the NPP ground system and NOAA processing system. The OMPS instrument performance is excellent and the provisional status of OMPS SDR products from the SNPP Interface Data Processing Segment (IDPS) is expected in spring 2013.

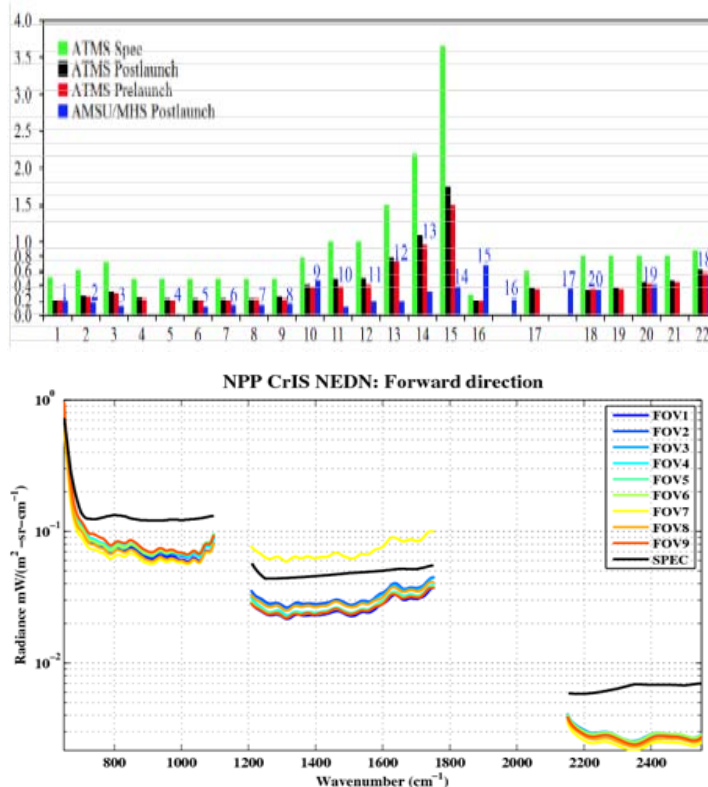


Figure 1. Top: ATMS Noise Equivalent Differential Temperature (NEDT) in comparison with AMSU-A/MHS. The ATMS channel number is indicated on the x-axis and the AMSU channel number is indicated in the figure in blue (Weng *et al.*, 2012). Bottom: CrIS Noise Equivalent Differential Radiance (NEDN) as a function of wave-number and Field of View (FOV).

Table 1. VIIRS performance met the specification. Signal to noise ratio is used for the reflective spectral band and NEDT is used for the thermal emissive band. The on-orbit performance and uncertainty are averaged from AeroSpace, NASA, and NOAA/STAR teams.

			Specification							Prelunch	On Orbit		
	Band No.	Driving EDR(s)	Spectral Range (um)	Horiz Sample Interval (km) (track x Scan)		Band Gain	Ltyp or Ttyp (Spec)	Lmax or Tmax	Spec SNR or NEDT (K)	Measured SNR or NEDT (K)	Measured SNR or NEDT (K)	Uncertainty	
				Nadir	End of Scan								
Reflective Bands	VisIR	M1	Ocean Color Aerosol	0.402 - 0.422	0.742 - 0.259	1.60 x 1.58	High	44.9	135	352	616.8	583	5
							Low	155	615	316	1092	1009	35
		M2	Ocean Color Aerosol	0.436 - 0.454	0.742 - 0.259	1.60 x 1.58	High	40	127	380	622.4	568	4
							Low	146	687	409	1118	992	17
		M3	Ocean Color Aerosol	0.478 - 0.498	0.742 - 0.259	1.60 x 1.58	High	32	107	416	690	619	8
							Low	123	702	414	1111	995	7
		M4	Ocean Color Aerosol	0.545 - 0.565	0.742 - 0.259	1.60 x 1.58	High	21	78	362	581.1	528	6
							Low	90	667	315	963.2	851	5
		I1	Imagery EDR	0.600 - 0.680	0.371 - 0.387	0.80 x 0.789	Single	22	718	119	240.7	214	1
		M5	Ocean Color Aerosol	0.662 - 0.682	0.742 - 0.259	1.60 x 1.58	High	10	59	242	366.6	328	7
							Low	68	651	360	827.9	652	21
	M6	Atmosph. Correct.	0.739 - 0.754	0.742 - 0.776	1.60 x 1.58	Single	9.6	41	199	415.2	361	6	
	I2	NDVI	0.846 - 0.885	0.371 - 0.387	0.80 x 0.789	Single	25	349	150	304.1	257	6	
	M7	Ocean Color Aerosol	0.846 - 0.885	0.742 - 0.259	1.60 x 1.58	High	6.4	29	215	519.8	446	11	
						Low	33.4	349	340	845.6	633	2	
	Emissive Bands	S/WMIR	M8	Cloud Particle Size	1.230 - 1.250	0.742 x 0.776	1.60 x 1.58	Single	5.4	165	74	273	227
M9			Cirrus/Cloud Cover	1.371 - 1.386	0.742 x 0.776	1.60 x 1.58	Single	6	77.1	83	253	229	2
I3			Binary Snow Map	1.580 - 1.640	0.371 x 0.387	0.80 x 0.789	Single	7.3	72.5	6	172	149	0
M10			Snow Fraction	1.580 - 1.640	0.742 x 0.776	1.60 x 1.58	Single	7.3	71.2	342	714	568	18
M11			Clouds	2.225 - 2.275	0.742 x 0.776	1.60 x 1.58	Single	0.12	31.8	10	25	22	0.1
I4			Imagery Clouds	3.550 - 3.930	0.371 x 0.387	0.80 x 0.789	Single	270	353	2.5	0.4	0.4	0
M12			SST	3.660 - 3.840	0.742 x 0.776	1.60 x 1.58	Single	270	353	0.396	0.13	0.13	0
M13			SST Fires	3.973 - 4.128	0.742 x 0.259	1.60 x 1.58	High	300	343	0.107	0.04	0.04	0.001
						Low	380	634	0.423				
LWIR		M14	Cloud Top Properties	8.400 - 8.700	0.742 x 0.776	1.60 x 1.58	Single	270	336	0.091	0.06	0.055	0.005
	M15	SST	10.263 - 11.263	0.742 x 0.776	1.60 x 1.58	Single	300	343	0.07	0.03	0.03	0	
	I5	Cloud Imagery	10.500 - 12.400	0.371 x 0.387	0.80 x 0.789	Single	210	340	1.5	0.4	0.4	0	
	M16	SST	11.538 - 12.488	0.742 x 0.776	1.60 x 1.58	Single	300	340	0.072	0.04	0.03	0	

During the intensive calval, the SDR teams have developed many innovative techniques for characterizing the instrument performance and improving the bias corrections. Numerous SDR processing bugs are fixed and the data quality flags are corrected and monitored at NOAA's instrument long-term monitoring system. The critical SNPP calval tasks have been completed.

(By Dr. F. Weng, [NOAA])

REFERENCES

Weng, F., X. Zou, X. Wang, S. Yang, M. Goldberg, 2012: Introduction to Suomi NPP ATMS for NWP and tropical cyclone applications, *J. Geophys. Res.*, doi:10.1029/2012JD018144.

Metop-B NOAA Instruments On-Orbit Performance Verification and Cal/Val Test

The Meteorological Operational (METOP)-B spacecraft was launched on September 17, 2012, and the on-board NOAA instruments were activated within a month after the launch. As part of the Initial Joint Polar System (IJPS), the National Environmental Satellite, Data, and Information Service (NESDIS) of the National Oceanic and Atmospheric Administration (NOAA) supports NOAA instrument operation through its Polar-orbiting Operational Environmental Satellites (POES) program. With the collaboration of EUMETSAT, the post-launch tests are performed for on-orbit verification (OV), and calibration and validation (Cal/Val). MetOp-B NOAA instruments (AMSU, AVHRR, and HIRS)

on-orbit verifications (OV) started on September 24, 2012 and the tests in Table 1 have been completed, including nine tests for AMSU, 12 for AVHRR and 12 for HIRS. In phase I, the tests focus on the instrument performance and response verification and were reported in daily meetings. The instrument performance is as expected and the post-launch noise performance meets the specifications, as shown in Figure 1. The phase II Cal/Val tests were performed to enhance the calibration accuracy and data quality. The results were presented and discussed in weekly meetings. NOAA/NESDIS/STAR hosted a review meeting on November 28, 2012, with participants from NOAA, NASA, and EUMETSAT, and the Cal/Val teams and product groups presented their test results. The instrument performance verifications from independent Cal/Val tests and data quality assessments from a variety of products are crucial for the enhancement of the quality of the data and products. The NOAA/STAR product groups have extended the Community Radiative Transfer Model (CRTM) and other product algorithms to MetOp-B NOAA instrument data and established the MetOp-B monitoring system to verify product consistency. The high sensitivity of the selected products to the radiometric calibration and geo-location correction facilitates feedback to the Cal/Val teams. The collaboration of the Cal/Val activities between NOAA and EUMETSAT is very important for Level 1B data exchange and data processing comparisons.

A MetOp-A and MetOp-B inter-comparison with correction of the Bidirectional Reflectance Distribution Function (BRDF) effect has been performed for AVHRR and HIRS visible and near-infrared channels. These two satellites are in the same orbit, one-half orbit time (~50 minutes) apart. Calibration updates for the AVHRR visible and near-infrared channels have been performed and are ready for delivery. To verify the accuracy of the brightness temperature measurements, a MetOp-A and MetOp-B inter-comparison is performed for AVHRR and HIRS infrared channels using the double difference method based on CRTM modeling of radiances. Further tests are also planned to enhance calibration accuracy and data quality, such as AVHRR/IASI and HIRS/IASI inter-comparisons for bias investigations.

(By Dr. T. Chang [NOAA]. The tests are performed by NOAA/NESDIS/STAR Cal/Val team, Drs. Fuzhong Weng, Xianqian Wu, Changyong Cao, Tsan Mo, Tiejun Chang, Chengli Qi, and Ding Liang with contributions from NOAA/NESDIS/STAR product groups and collaboration with EUMETSAT)

Table 1. On-Orbit (OV) tests for NOAA instruments on MetOp-B

AMSU	HIRS	AVHRR
A/C Conv. Evaluation	BB temperature measurement	General evaluation of imagery
Space/Warm View Interference	Dark current restore	Instrument stability and trending
Instrument Trending	IR channel instrument noise	Clamp stability
Scanner Accuracy & Stability	VIS channel noise and dynamic range	IR channel noise and dynamic range
Optimal Space view position	Calibration slope	VIS channel instrument noise
Noise measurement (NEAT)	Calibration intercept	IR calibration slope
Inter-Satellite Comparison	Assessment by CRTM	Image striping
Blackbody PRT Temp accuracy	Visible channel assessment	Geo-location verification
Earth Scene Bias Characterization	Geo-location evaluation	VIS channels calibration
	Instrument temperature	VIS channels consistency
	Coherent noise	Stray light
	Stray Light	IR Radiances Assessment

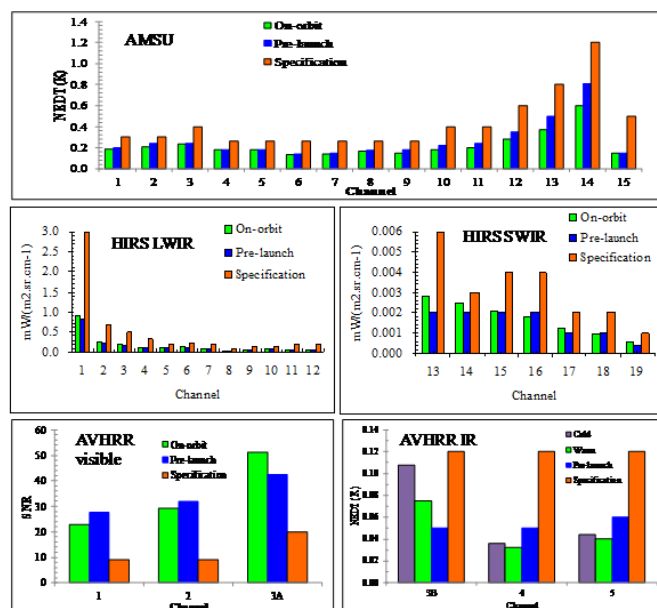


Figure 1. Metop-B NOAA instrument noise performance. Top: AMSU noise equivalent differential temperature (NEDT). Middle: HIRS noise equivalent differential radiance (NEDN). Bottom: AVHRR visible channel Signal to Noise Ratio (SNR) and IR channel NEDT.

Using Variograms to Quantify the Radiometric Stability of Meteosat-7/MVIRI and Metop-A/HIRS by Inter-comparison with Metop-A/IASI

Fundamental Climate Data Records (FCDRs) are long-term data records of calibrated and quality-controlled sensor data designed to allow the generation of homogeneous products that are accurate and stable enough for climate monitoring. The generation of FCDRs from multiple instruments relies on their accurate inter-calibration. Where the calibration is transferred backwards or forwards in time by a single instrument, the long-term radiometric stability of that instrument becomes a direct contribution to the uncertainty in the FCDR.

It is difficult to quantify the long-term stability of an instrument's calibration, based on a time series of comparisons with a reference, because changes to the reference must be accounted for. If the reference is another instrument, its long-term radiometric stability must also be accounted for, as well as any orbital changes, such as drift in equator crossing time, which can alias diurnal calibration variations. If the reference is a Numerical Weather Prediction (NWP) model, we need to account for not only changes to the model itself, but also all the observations it uses and its assimilation system. This limits the application of NWP as a long-term calibration reference, although some of these shortcomings can be addressed by using NWP models to generate reanalysis datasets.

The Metop-A satellite has operated since 2006 in a stabilised sun-synchronous polar orbit where the local 21:30 equator crossing time is held constant. Metop-A carries the Infrared Atmospheric Sounding Interferometer (IASI), which has been shown to have excellent radiometric stability (EUMETSAT Tech Report, 2011) and can provide a good inter-calibration reference against which the stability of other instruments can be assessed.

Metop-A also carries a High-resolution Infrared Sounder (HIRS). Different generations of these instruments have been operated on various polar platforms since 1978, which makes them interesting potential reference instruments for the inter-calibration of the infrared channels of geostationary imagers, such as Meteosat. The big advantage of both HIRS and IASI being operated on Metop-A is that it is easy to generate a very large dataset of collocations from their observations.

In this analysis the stability of observations from the HIRS on-board Metop-A, and Meteosat Visible and InfraRed Imager

(MVIRI) on-board Meteosat-7, is evaluated against reference observations from the IASI instrument on-board Metop-A. The analysis takes the 2008-2012 time series of biases evaluated for standard scene radiances from the inter-comparison of these instruments as described in (Hewison, 2008). The analysis focuses on the “infrared” and “water vapour” channels of MVIRI, which correspond to Channel 8 (~6.5 μm) and Channel 12 (~11.5 μm) of HIRS respectively.

We introduce the concept of the temporal variogram, $2\gamma_t(\Delta t)$, which is calculated between brightness temperatures biases, ΔT_b , sampled at different intervals, Δt , from an extended time series, $\Delta T_b(t)$, following the method outlined in (Hewison, 2013) and (Hewison, 2009):

$$2\hat{\gamma}_t(\Delta t) = \frac{1}{n_i} \sum_i [\Delta T_b(t_i + \Delta t) - \Delta T_b(t_i)]^2 \quad (1)$$

Figure 1 shows the temporal variograms evaluated for two channels of Metop-A/HIRS using Metop-A/IASI as a reference over periods from 1d to 1000d. These channels were chosen as they are most representative of the “water vapour” and “infrared” channels of Meteosat/MVIRI. Their variograms characteristically increase with time rapidly for periods up to 29 d, which corresponds to the averaging period used to generate the prototype inter-calibration products. Beyond this limit, the variograms of the water vapour channel increase more slowly, reaching $(2\gamma_t)^{1/2} = 33.8 \pm 2.2$ mK for periods of 1 year. The variograms for the infrared channel show a strong maximum for periods ~6 months, indicating an annual cycle in the time series and reach minima of 9.0 ± 0.6 mK for periods of 1 year, with a further clearly-defined minimum at $\Delta t = 2$ yr.

These results demonstrate that radiometric calibration of Metop-A/HIRS was sufficiently stable over this period that it is unlikely to contribute significantly to the overall uncertainty of the inter-calibration of geostationary imagers compared to uncertainties in the spectral band adjustment. However, these results may not be directly transferable to HIRS on other platforms, which suffer from equator crossing time drift.

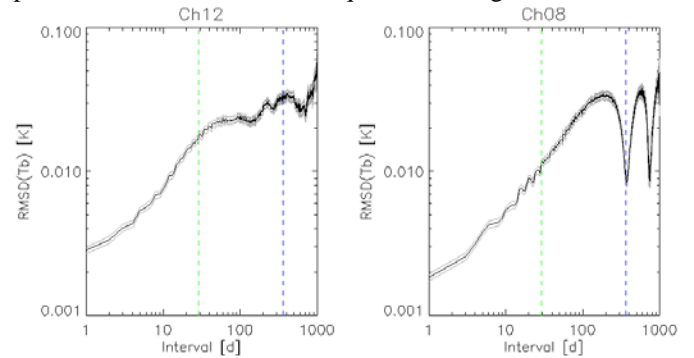


Figure 1 – Temporal variograms $[(2\gamma_t)^{1/2}]$ calculated as RMS differences in Standard Biases for Ch12 and Ch8 of Metop-A/HIRS calculated with reference to Metop-A/IASI. Vertical lines show periods of 29d and 1yr.

It is interesting to compare the above results with those from a similar analysis of a comparable time series of standard biases from the inter-calibration of Meteosat-7/MVIRI using Metop-A/IASI, based on the algorithm described in (Hewison *et al.*, 2013). The variograms for the water vapour and infrared channels, in Figure 2, show the same characteristic increase for periods from 1 – 29 d. In this case, the water vapour channel shows a clear annual cycle, with a maximum for periods ~6 months, but reaching a minimum of $(2\gamma_i)^{1/2} = 65.0 \pm 4.1$ mK for $\Delta t = 1$ yr. However, the infrared channel also shows a twice yearly oscillation, and its variogram reaches 187 ± 12 mK for $\Delta t = 1$ yr. Both variograms are much higher, both in their *nugget value* (offset) and in their *sill value* (maximum), than those of their counterpart channels on HIRS, confirming that using HIRS as an inter-calibration reference could improve FCDRs derived from Meteosat-7. The higher nugget value can be explained by uncertainties caused by collocation errors between the MVIRI and IASI observations. The high sill value indicates that the water vapour and infrared channels of MVIRI drift faster from IASI than the corresponding HIRS channels.

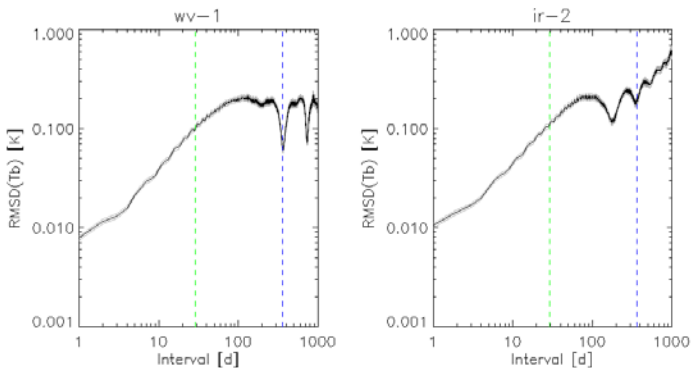


Figure 2 – As Figure 1, but for Water Vapour (left) and InfraRed (right) channels of Meteosat-7/MVIRI.

In conclusion, this analysis indicates that the Metop-A/HIRS may serve as stable reference for the re-calibration of the water vapour and infrared channels on-board geostationary satellites. The fact that the MVIRI channels reveal a larger drift than the HIRS channels suggests that MVIRI may not be stable enough to serve as bridge between different NOAA satellites.

(By Drs. T. J. Hewison and R. Roebeling, [EUMETSAT])

REFERENCES

- EUMETSAT Technical Report, 2011: GSICS Traceability Statement for IASI and AIRS, [EUM/MET/TEN/11/0157](http://www.eumetsat.org/Portals/0/EUMETSAT/TEN/11/0157)
 Hewison, T., 2008: MetOp-A IASI and HIRS Inter-Comparisons At EUMETSAT”, *GSICS Quarterly*, **2(3)**.

- Hewison, T., 2013: An Evaluation of the Uncertainty of the GSICS SEVIRI-IASI Inter-Calibration Products. *IEEE Trans. Geosci. Remote Sensing*, in press.
 Hewison, T. 2009: Quantifying the Impact of Scene Variability on Inter-Calibration, *GSICS Quarterly*, **3(2)**.
 Hewison, T.J, X. Wu, F. Yu, Y. Tahara, X. Hu, D. Kim and M. Koenig, 2013: GSICS Inter-Calibration of Infrared Channels of Geostationary Imagers using Metop/IASI, *IEEE Trans. Geosci. Remote Sensing*, in press.

The Development of AMSU FCDR's and TCDR's for Hydrological Applications

This NOAA/NCDC/CDR Program project will properly characterize the AMSU and MHS sensors to generate FCDR's from the Advanced Microwave Sounding Unit (AMSU) and Microwave Humidity Sounder (MHS): channels 1, 2, 3 and 15 on AMSU-A and all five channels on AMSU-B and MHS. The FCDR's will then be used to generate TCDR's for hydrological cycle products such as precipitable water, rain rate and snow cover, etc. By project completion, an 11-year (2000 – 2010) AMSU/MHS CDR from NOAA POES satellites (NOAA-15 to -19) and EUMETSAT Metop-A satellite is anticipated. This three-year project is currently in its final year and has met many of its major milestones. Two advances are described below: geolocation correction and scan bias correction for AMSU-A window channels.

The accuracy of sensor geolocation is affected by errors in satellite attitude (pitch, roll, and yaw, or PRY), sensor mounting, and satellite clock offset, etc. Geolocation error can be a significant source of bias in satellite measurements of geographical areas with sharp T_b gradients. In this project, geolocation error was quantified with the difference between ascending and descending brightness temperatures (ΔT_b) along coastlines. With the existence of geolocation error ΔT_b along the coastlines becomes the difference between land and ocean T_b 's. This difference is quite significant for surface sensitive frequencies due to the large difference between land and water emissivity. The PRY corrections were derived by tuning satellite attitudes (PRY) until the number of coastal pixels exceeding a preset ΔT_b threshold was minimized (Moradi *et al.*, 2012). New geographical coordinates, scan angle, and local zenith angles were then calculated using the new attitudes. The results show that NOAA-15 AMSU-A2 sensor is mounted about 1.2 degrees negative cross-track, and about 0.5 degree negative along-track; NOAA-16 AMSU-A1 and -A2 are mounted about 0.5 degree negative along-track, and NOAA-18 AMSU-A2 is mounted more than 1 degree negative along-track. Figure 1 compares the ΔT_b before and after geolocation correction for NOAA-15 AMSU-A 23.8 GHz.

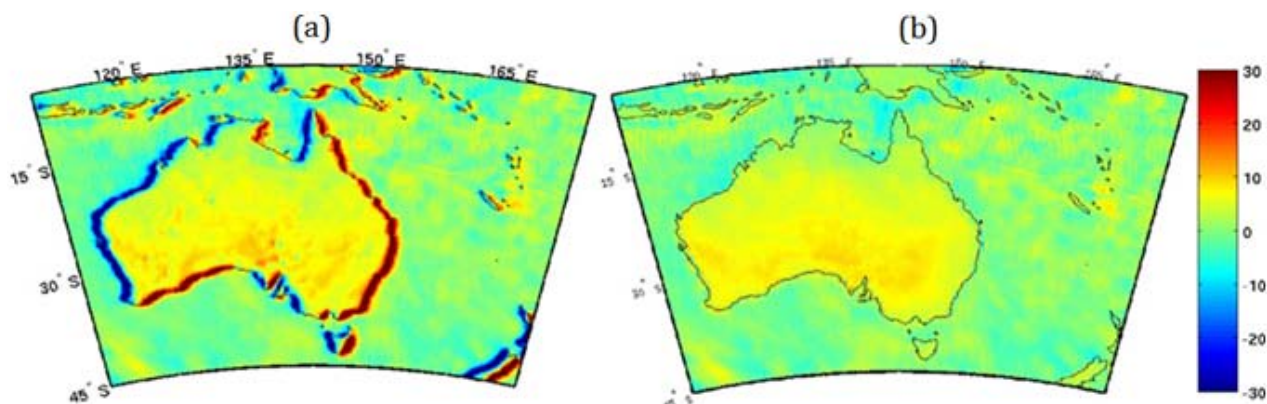


Figure 1. Difference between ascending and descending brightness temperatures from NOAA-15 AMSU-A 23.8 GHz channel, (a) before correction; and (b) after correction.

AMSU-A window channels are known for their cross scan asymmetry issues (Weng *et al.*, 2003). If not corrected, the bias will have a severe impact on the generation of geophysical products. Several approaches were used in this project to quantify the scan biases for AMSU-A channels 1, 2, 3, and 15 (respectively at 23.8, 31.4, 50.3, and 89 GHz). These include vicarious cold reference (VCR) over ocean, VCR over certain land target areas in the polar regions, vicarious hot reference (VHR) over a target area in Amazon, and Most Probable Value (MPV) over ocean. MPV is defined as narrow ranges of modeled sea surface temperature, precipitable water, and wind speed that have the highest frequency of occurrence in the data set. Since the scan bias appears to be T_b dependent, different methods were employed to cover the dynamic ranges of the T_b 's. The coldest T_b for channels 1 and 2 are over ocean while for channels 3 and 15 they are over land. Consequently, VCR over ocean was used in the bias characterization for channels 1 and 2, and VCR over land for channels 3 and 15. The bias patterns appeared to be stable for the same satellite through the several years of data examined, but were quite dissimilar for the different satellites. Based on the bias characterization, a three-point approach is developed to correct the scan bias for each channel at each beam position (Yang *et al.*, 2012). The method appears to remove the scan bias effectively for AMSU-A window channels both at brightness temperature level and at product level. Figure 2 (below) compares the Cloud Liquid Water (CLW) retrieved using the AMSU-A channels 1 and 2 T_b 's before and after

scan bias correction. The asymmetry in CLW caused by the scan bias in T_b was clearly removed after the bias correction especially along the limbs.

(by H. Meng, R. Ferraro, W. Yang, I. Moradi, and C. Divaraj, [NOAA])

REFERENCES

- Moradi, I., H. Meng, R. Ferraro, S. Bilanow, Correcting geolocation errors for microwave instruments aboard NOAA satellites. *IEEE Transactions on Geoscience and Remote Sensing*, doi:10.1109/TGRS.2012.2225840.
- Weng, F., L. Zhao, R. R. Ferraro, G. Poe, X. Li, and N. C. Grody (2003), Advanced microwave sounding unit cloud and precipitation algorithms. *Radio Sci.*, 38 (4), 8068, doi:10.1029/2002RS002679.
- Yang, W., H. Meng, R. Ferraro, I. Moradi, C. Devaraj, Cross scan asymmetry of AMSU-A window channels: characterization, correction and verification. *IEEE Transactions on Geoscience and Remote Sensing*, doi:10.1109/TGRS.2012.2211884.

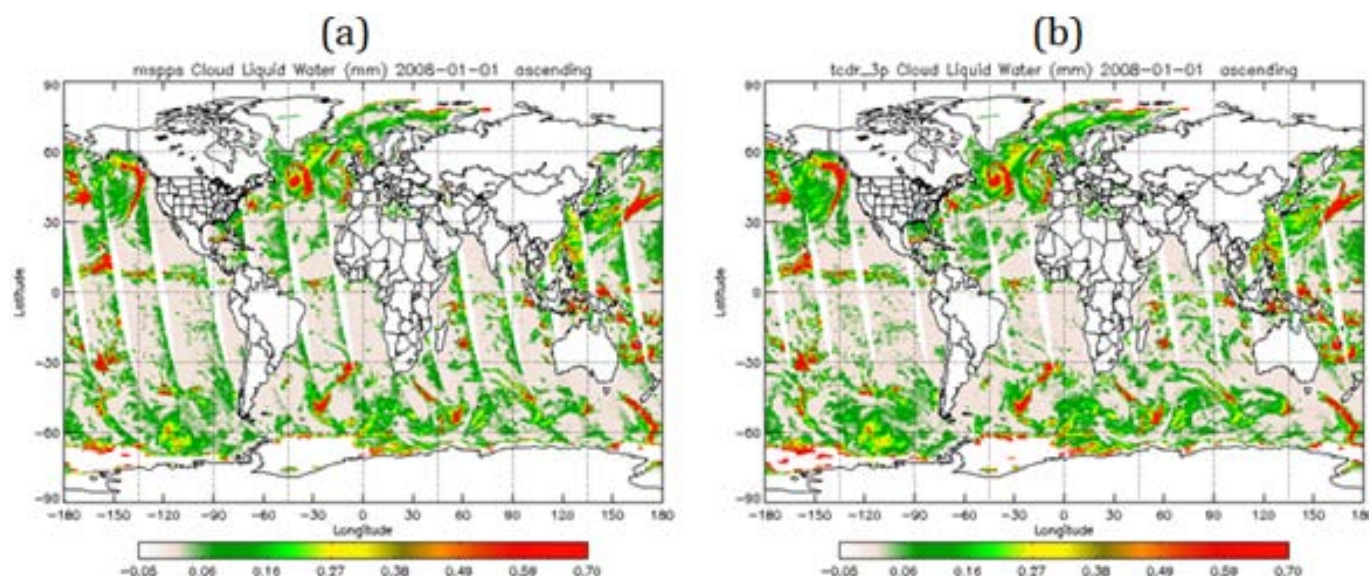


Figure 2. Cloud liquid water retrieved from AMSU-A channels 1 and 2 measurements before (a) and after (b) scan bias correction.

News in this Quarter

Two GSICS GEO-LEO IR Correction Products in Pre-operational Phase

On behalf of the GSICS Coordination Center (GCC) and GSICS Product Acceptance Team (GPAT), I am pleased to announce that the EUMETSAT GSICS GEO-LEO IR inter-calibration correction product for Meteosat/SEVIRI and the NOAA GSICS GEO-LEO IR inter-calibration correction product for GOES Imager are now in pre-operational phase. These two products have completed the required documentation including the Algorithm Theoretical Basis Document (ATBD), uncertainty analysis and other ancillary reports. The software for these two products is running stably and reproducibly with minimal code changes expected. The software for the NOAA product has been maintained with the subversion control package. The product data availability and metadata have also been running reliably and stably at the GSICS data servers over the past years. We have received some positive feedback from product users and continue to encourage user comments. Per the GSICS Procedure for Product Acceptance (GPAA) (<https://gsics.nesdis.noaa.gov/wiki/Development/GppaWorkflow>) and the SCOPE-CM maturity model

(<http://www.agu.org/pubs/crossref/2012/2012EO440006.shtml>), these two products are now in pre-operational phase, on the way to operations.

Users can access to the products and the associated documents freely at the GSICS product catalog at <http://www.star.nesdis.noaa.gov/smcd/GCC/ProductCatalog.php>, which is also linked to the WMO GSICS portal website.

(by F. Yu, [GCC])

Current Status of Meeteosat-9 and -10

During 2012, Met9 was located at 0° and provided a Full Earth Scan (FES) service of the earth, with images every 15 minutes. It also provided a Low Rate Information Transmission (LRIT) direct service, Data Collection Platform (DCP) service, and Search and Rescue (SAR) service.

MSG3 (Met10) was launched on 5 July 2012 and handed over by ESOC to EUMETSAT on 16 July 2012. The spacecraft, located at 3.4° west, has successfully completed commissioning. MSG3-SEVIRI was successfully switched ON with a first image on 7 August 2012 and MSG3-GERB was successfully switched ON with a first image on 10 August 2012. The MSG-SAR payload entered operation in September 2012. MSG has been disseminating test Image and Product data to users since late October 2012 and was renamed Met10 in mid-December 2012. Met10 commenced an operational

FES service of the earth in parallel with Met9 on 19-December 2012. During this two month parallel operation, Met10 will take over the 0° FES service as the prime spacecraft.

(By T. Hewison [EUMETSAT])

NetCDF Formats from the EUMETSAT Data Centre

The EUMETSAT Data Centre is offering the NetCDF format as a common delivery format for Metop-A and in the near future, Metop-B level 1 and 2 products. In the scope of GSICS, this is good news as the products' NetCDF formats follow the same GSICS NetCDF recommendations *i.e.* product filenames conform to the WMO file naming conventions, adopting Climate and Forecast (CF) conventions for "Coordinate Types", and using CF standard names and units where applicable.

Users are encouraged to use these product formats in future GSICS activities and provide feedback to EUMETSAT via ops@eumetsat.int. More information regarding these products can be found under the following URL:

http://www.eumetsat.int/Home/Main/DataAccess/EUMETSATDataCentre/SP_20111027152034196?l=en

(By P. Miu, [EUMETSAT])

Just Around the Bend...

GSICS-Related Meetings

- The annual GRWG and GDWG joint meeting will be held in Williamsburg, Virginia, USA on 4-8 March 2013.
- The 5th GSICS Users' Workshop will take place in conjunction with the first NOAA Satellite Conference which will be held in College Park, Maryland, USA, April 8-12, 2013. Remote access to the users' workshop will be available via Webex.
- The first NOAA Satellite Conference will be held at the NOAA Center for Weather and Climate Prediction (NCWCP), College Park, USA April 8-12, 2013.

GSICS Publications

Gowarda, S., et al., 2012: Complementarity of ResourceSat-1 AWiFS and Landsat TM/ETM+ sensors. *Remote Sensing of Environment*, **123**, 41-56.

Hu, X., et al., 2012: Calibration for the solar reflective bands of Medium Resolution Spectral Imager onboard FY-3A. *IEEE Trans. Geoscience and Remote Sens.*, **50(12)**, 4915-4928.

Jin, T., et al., 2012: Cross-calibration and errors analysis of ionosphere correction in satellite altimetry. *Geometrics and Information Science of Wuhan University*, **37(6)**, 658-661.

Kamei, A., et al., 2012: Cross calibration of Formosat-2 Remote Sensing Instrument (RSI) using Terra Advanced Spaceborne Thermal Emission and Reflection Radiometer (ASTER). *IEEE Trans. Geoscience and Remote Sens.*, **50(11)**, 4821-4831.

Pahlevan, N., and J. Schott, 2012: Characterizing the relative calibration of Landsat-7 (ETM+) visible bands with Terra (MODIS) over clear waters: the implications for monitoring water resources. *Remote Sensing of Environment*, **125**, 167-180.

Wang, W., et al., 2012: Cross-calibration of the Total Ozone Unit (TOU) with the Ozone Monitoring Instrument (OMI) and SBUV/2 for environmental applications. *IEEE Trans. Geoscience and Remote Sens.*, **50(2)**, 4943-4955.

Smith, A., et al., 2012: Lunar Spectral Irradiance and Radiance (LUSI): new instrumentation to characterize the Moon as a space-based radiometric standard. *Journal of Research of the National Institute of Standards and Technology*, **117**, 185-201.

Xu, N., et al., 2012: Cross-calibration of FY-2E/VISSR infrared window and water vapor channels with Terra/MODIS. *Journal of Infrared and Millimeter Waves*, **31(4)**, 319.

With Help from our Friends:

The *GSICS Quarterly* Editor would like to thank those individuals who contributed articles and information to this newsletter. The Editor would also like to thank Dr. George Ohring for careful proofreading and editing assistance, our European Correspondent, Dr. Tim Hewison of EUMETSAT, and Asian Correspondent, Dr. Yuan Li of CMA, in helping to secure and edit articles for publication.

Submitting Articles to GSICS Quarterly: The *GSICS Quarterly* Press Crew is looking for short articles (<1 page), especially related to cal/val capabilities and how they have been used to positively impact weather and climate products. Unsolicited articles are accepted anytime, and will be published in the next available newsletter issue after approval/editing. **Please send articles to Fangfang.Yu@noaa.gov.**